

We are IntechOpen, the world's leading publisher of Open Access books Built by scientists, for scientists

6,900

Open access books available

186,000

International authors and editors

200M

Downloads

Our authors are among the

154

Countries delivered to

TOP 1%

most cited scientists

12.2%

Contributors from top 500 universities



WEB OF SCIENCE™

Selection of our books indexed in the Book Citation Index
in Web of Science™ Core Collection (BKCI)

Interested in publishing with us?
Contact book.department@intechopen.com

Numbers displayed above are based on latest data collected.
For more information visit www.intechopen.com



Calculation of the Metastable Atom Densities in Argon and Neon Abnormal Glow Discharges

Abdelaziz Bouchikhi

Abstract

In this chapter an investigation of a DC argon and neon abnormal glow discharges with metastable atom density is presented. The values of pressure are between 133.32 and 330 Pa, and the voltage range is from 250 to 400 V in the case of argon gas. In the case of neon gas, the pressure has the value of 399.92 Pa (3 Torr) and the voltage ranges from 300 to 500 V. In the frameworks, an analysis of abnormal glow discharge characteristics is carried out in the case of input data taken from the Boltzmann equation in multi term approximation (BMA), and in the case of input data obtained from BOLISG+ code. As conclusion of these differences of input data in the same gas the output results are different and it appears in the cathodic region. The spatiotemporal distributions of electron and ion densities, the potential and electric field, the mean electron energy and the metastable atom density are shown. A 1D fluid model is used to solve self-consistently the first three moments of the Boltzmann's equation coupled with the Poisson's equation. Our results are validated with those obtained by both recent paper and experimental results.

Keywords: metastable atom density, abnormal glow discharge, fluid model, input data

1. Introduction

The concern of the amelioration of the plasma reactor is always a domain important in the development technology, among these fields we find glow discharge. A plasma technology in a gas mixture has been studied by several authors. Ono et al. [1] have been studied oxygen-nitrogen gas mixture glow discharge plasma by intervene many chemical reactions in their model. Khomich et al. [2] have been treated the problem of the atomic deposition in the metal surface modification by nitrogen-argon mixture glow discharge in abnormal regime. Ponduri et al. [3] have been analyzed the dissociation of CO₂ by dielectric barrier glow discharge, as a consequence of utilization of CO₂ gas a lot of kinds of species intervene in the phenomena discharge. Baadj et al. have been [4] investigated Xe-Cl₂ gas mixture for the formation of XeCl* exciplex lamp by means of zero-dimensional model. Li et al. [5] have been studied the plasma jet length in Ne, Ar, He and Kr in atmospheric pressure when the excimer molecule formatted from

metastable state of the atomic gases, and they have been identified three modes versus of the gas flow rate, its about laminar, transition, and turbulent jet modes.

In this chapter, an research is through concerning the role of neon and argon metastable atoms in the discharge. Metastable atoms have been considered by several authors, both theoretically and experimentally. Metastable densities can experimentally be measured by optical absorption method. In theoretical means, a poise equation, including different production and loss terms is assembled to compute the metastable densities. Experimental measurements were executed, for example, for Neon gas in an RF glow discharge by Eckstein et al. [6], for Ar gas in a microwave boosted glow discharge by Uzelac and Leis [7], and for He gas as a function of discharge conditions by Browne and Dunn [8]. In the research of Smith et al. [9] purely relative absorption signals of Argon metastable atoms as a function of current and pressure were experimented. In the research of Strauss et al. [10] and Ferreira et al. [11] Argon metastable densities were experimented in a afterglow of a pulsed discharge and in the Grimm-type glow discharge, respectively, and some mechanisms for the structure of Argon metastable atoms were recommended. Argon metastable densities have also been experimented by Ferreira et al. [12], and by Ferreira and Ricard [13].

A comparison was complete with Argon metastable densities determined from a coupled-electron-metastable-atom model. Hardy and Sheldon [14] have examined Argon, Helium and Neon gases. A comparison between calculated and measured metastable densities was also realized by Kubota et al. [15] for Helium in a RF and DC glow discharge. Lymberopoulos and Economou [16] have established a combined fluid model for the electrons, Ar metastable atoms, and Ar ions in order to study the effect of metastable atoms in the discharge. In the works [17–22] rate constants of a number of collision processes in control of the demolition of metastable atoms were got by combining equilibrium equations with the experimented time-dependent variation of the metastable densities or by analyzing the reliance of the decay constants upon pressure. Den Hartog et al. [23, 24] have investigated Helium gas.

Last-mentioned, Fedoseev and Sukhinin [25] have investigated the influence of metastable Ar atoms on gas discharge plasma with dust particles. Shumova et al. [26] have investigated the effect of metastable Ne atoms and dust particles in a positive column of glow discharge.

The aim of this work is to present, influence of the discharge characteristic in the case of input data obtained by BOLSIG+ code, and in the case of input data taken from the Boltzmann equation in multi term approximation (BMA). We note that both these approaches are widely used. For simulations of positive column of glow discharge, Vasilyak et al. [27] used the first approach, while Sukhinin et al. [28] used the second approach. In Section 2, the mathematical model is delineated; it comprises the boundary and initial conditions as well as the numerical method. In Section 3, the results are discussed for Ar discharge. In Section 4, the test scheme is given. In Section 5, Influence of the input data got from BOLSIG+ on the argon discharge has been shown. In Section 6, the characteristics of the Ne discharge with input data taken from BOLSIG+ are presented. Finally, the conclusion of the chapter is given in Section 7.

2. Discharge modeling

Our mathematical model builds on the first three moments of the Boltzmann equation. The Continuity equations and momentum transfer equations of metastable atom, electrons and positively charged ions. The energy equation is known only

for electrons, and to give the effect of the electric field on the particles charged, the Poisson equation is included in the model [29, 30].

The chemical reactions intervene in the discharge are indicated in the **Table 1**.

After that, the model in the 1D Cartesian geometry, writes by partial differential equations:

$$\frac{\partial n_e}{\partial t} + \frac{\partial \varphi_e}{\partial x} = n_e (n_o K_o^{io} + n_m K_m^{io}) + n_m n_m K^{ci}, \quad (1)$$

$$\frac{\partial n_+}{\partial t} + \frac{\partial \varphi_+}{\partial x} = n_e (n_o K_o^{io} + n_m K_m^{io}) + n_m n_m K^{ci}, \quad (2)$$

$$\frac{\partial n_m}{\partial t} + \frac{\partial \varphi_m}{\partial x} = n_e (n_o K_o^m - n_m K_m^o - n_m K_m^{io}) - 2n_m n_m K^{ci} - \frac{n_m}{\tau_m}, \quad (3)$$

$$\frac{\partial \varepsilon_e n_e}{\partial t} + \frac{\partial \varphi_{ee}}{\partial x} = -e \varphi_e E + \varepsilon^m n_e n_m K_m^o + \varepsilon^{ci} n_m n_m K^{ci} - n_e P^{ec} - n_e (\varepsilon^m n_o K_o^m + \varepsilon^{io} n_o K_o^{io} + (\varepsilon^{io} - \varepsilon^m) n_m K_m^{io}), \quad (4)$$

$$\frac{\partial^2 V}{\partial x^2} = -\frac{e}{\varepsilon_o} (n_+ - n_e) \quad (5)$$

Here n_e , n_+ , n_m , φ_m , φ_e and φ_+ are number densities, densities of transport flux of the metastable atoms, electrons and ions, respectively. K_o^m is the rate coefficient of electron-impact excitation of ground state atoms, $\varepsilon^m = 11.55$ eV is the energy loss of excited atoms, n_o is the constant background gas density, K_m^{io} is the rate coefficient of electron-impact ionization of excited atoms with the energy loss ($\varepsilon^{io} - \varepsilon^m$), K_o^{io} is the rate coefficient of electron-impact ionization of ground state atoms and $\varepsilon^{io} = 15.76$ eV is the energy loss of ionized atoms, K_m^o is the rate coefficient of de-excitation of excited atoms by electron collisions. $E = -\partial V/\partial x$ is the electric field strength. ε_o and e are the permittivity of free space and elementary charge, respectively. $K^{ci} = 8.1 \times 10^{-10} \text{ cm}^3 \text{ s}^{-1}$ [31] is the rate coefficient of chemo-ionization processes with the energy gain $\varepsilon^{ci} = 2\varepsilon^m - \varepsilon^{io}$. $\tau_m = 1 \mu\text{s}$ is the metastable lifetime. ε_e is the mean electron energy, φ_{ee} is the electron energy flux. V is the electrostatic potential. P^{ec} is the energy loss per electron due to elastic collision of electrons with the background gas [32].

Momentum transfer equations for metastable atoms, electrons, ions and electron energy [33–35] are:

Processes	Name of processes
$\text{Ar} + \text{e}^- \rightarrow \text{Ar}^+ + 2\text{e}^-$	Ionization
$\text{Ar} + \text{e}^- \rightarrow \text{Ar}_m^* + \text{e}^-$	Excitation
$\text{Ar}_m^* + \text{e}^- \rightarrow \text{Ar} + \text{e}^-$	De-excitation
$\text{e}^- + \text{Ar}_m^* \rightarrow \text{Ar}^+ + 2\text{e}^-$	Stepwise ionization
$\text{Ar}_m^* + \text{Ar}_m^* \rightarrow \text{Ar}^+ + \text{e}^- + \text{Ar}$	Chemo-ionization

Table 1.
 Kinetic scheme of processes.

$$\varphi_e = -n_e \mu_e E - \frac{\partial D_e n_e}{\partial x}, \quad (6)$$

$$\varphi_+ = n_+ \mu_+ E - \frac{\partial D_+ n_+}{\partial x}, \quad (7)$$

$$\varphi_m = -D_m \frac{\partial n_m}{\partial x}, \quad (8)$$

$$\varphi_{ee} = -n_e E \mu_{ee} - \frac{\partial n_e D_{ee}}{\partial x} \quad (9)$$

Here μ_e , μ_+ , D_e and D_+ are the electron, ion for mobilities and diffusion coefficients, respectively. D_{ee} and μ_{ee} are the diffusivity and mobility of electron energy transport. The ion mobility has brought from Phelps and Petrović [36] and their ion diffusivity is computed agree with Einstein's relation [37]. The coefficients for electrons [38] in argon as dependences on the mean electron energy are got as of INP Greifswald for direct evaluation with the results obtained by Becker et al. [30]. D_m is the metastable atom diffusivity someplace $n_o D_m = 1.7 \times 10^{18} \text{ cm}^{-1} \text{ s}^{-1}$ [19].

2.1 Boundary and initial conditions

The discharge is affected between two parallel plate electrodes and the radius of the electrode is presumed to be higher than the electrode gap and the physical characteristic distributions are approximately uniform along the radial direction. The grounded electrode has been put at $x = 1 \text{ cm}$, play the role as the anode ($V_{anode} = 0$). The powered electrode has been put at $x = 0 \text{ cm}$, which initiates the model discretization, play the role as the cathode ($V_{cathode} = -V_{DC}$).

At time $t = 0$, the metastable atom, electron, and ion densities are supposed constant and equal to 10^3 cm^{-3} , and the mean electron energy equal to 1 eV .

Presuming disappearance of the metastable atom density, i.e., $n_m = 0$ has been arranged at the cathode, whilst a predominant field-driven flux shut to the cathode the expression $\partial D_+ n_+ / \partial x = 0$ has been used for the positive ion density $\forall t > 0$. At the anode, the metastable atoms and the electron density are supposed to be zero. The electron flux separating the cathode is calculated by the expression $\varphi_e(x = 0, t) = -\gamma \varphi_+(x = 0, t) \forall t > 0$, the mean electron energy is assumed to be 5 eV at the cathode [36] and the gas temperature is equal to 273 K in the discharge.

2.2 Numerical method

For the metastable atom and Poisson equations a finite difference method has been employed. The transport equations of the electron energy, electron and ion are also discretized spatially with the finite difference technique. In this method the exponential scheme has been employed into account [37, 39–42]. The discretization of the time terms by the right position of the finite difference technique has been used. Consequently, every discretized equation is defined as a tridiagonal matrix, which is solved by Thomas's algorithm.

3. Results and discussion of argon discharge

In this part, we will analysis the spatiotemporal evolution of the abnormal glow discharge in the existence of metastable atom density. The gas pressure is 133.32 Pa . The neutral species density is computed from the temperature and gas pressure with the ideal gas law. The constant value for the secondary electron yield is 0.06 [36].

The applied potential at the cathode is -400 V. The uniform subdivision of the space interval in 250 elements and a time step $\Delta t = 10$ ps, have been utilized.

Figure 1 shows the temporal progression of the potential (**Figure 1(a)**), concentration of electrons (**Figure 1(b)**), concentration of ions (**Figure 1(c)**), concentration of metastable atoms (**Figure 1(d)**), the electric field (**Figure 1(e)**) and the mean electron energy (**Figure 1(f)**). We remark that the discharge is distinguished by three zones: the first one busied the time simulation amidst in 10^{-11} and 9×10^{-6} s, the second one took the time simulation inter-time of 9×10^{-6} and 3×10^{-5} s, the final zone busied the time simulation amidst in 3×10^{-5} and 3.6×10^{-5} s.

For the first zone, we comment that the metastable atom, electrons and ion concentrations are almost identical. Therefore, the net space charge concentration is unimportant. The electric potential is distinguished by the Laplace form due to the net space charge concentration that is exist. Consequently, the electric field is seemingly constant, besides that the mean electron energy is constant.

In the second zone, we remark a pseudo emergence of the cathodic region, this is characterized by a significance of ion concentration and unimportant of the electron

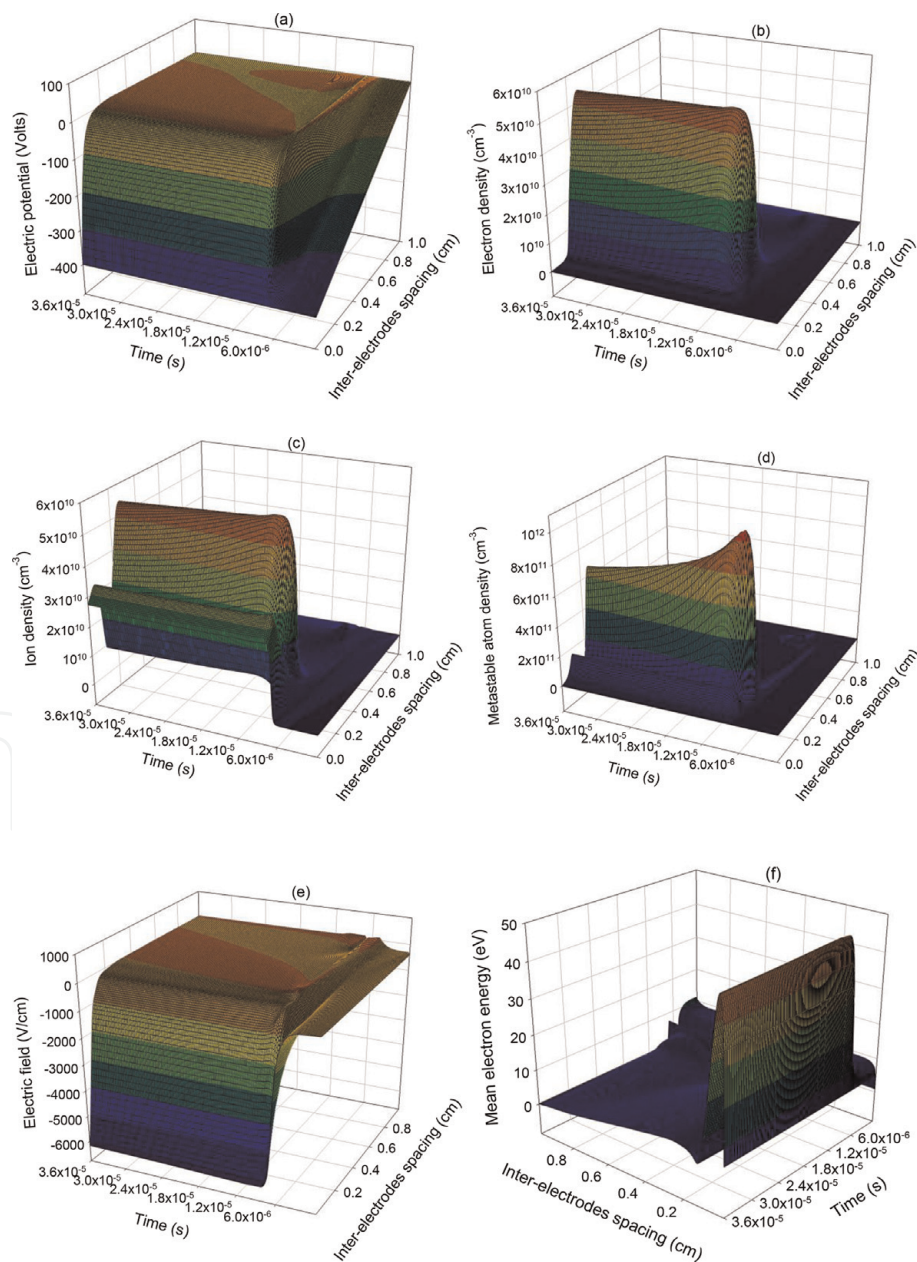


Figure 1. Argon spatiotemporal distributions of electric potential (a), electrons volume number (b), ions volume number (c), metastable atom density (d), electric field (e), and mean electron energy (f) at 400 V.

concentration. This is explicated by the velocity of the electron species, which speed a more than the ion species and displaced quickly starting at the cathodic region. Consequently, the amount ($n_e - n_+$) is considerable which influence directly the electric potential as consequence the important chute that is present. Inevitably, the electric field is intense. The last earns the electron species an important energy. We comment that the metastable atom concentration is important. This discharge is sustained by the secondary emission coefficient as well as the existence of metastable atom concentration. Sooner than $t = 3 \times 10^{-5}$ s we remark a pseudo emergence of the negative glow region, where it is typified by the similar electron and ion concentrations. Consequently the net space charge concentration is slight. Hence, the electric potential and the electric field are constants. Automatically, the metastable atoms concentration is diminished.

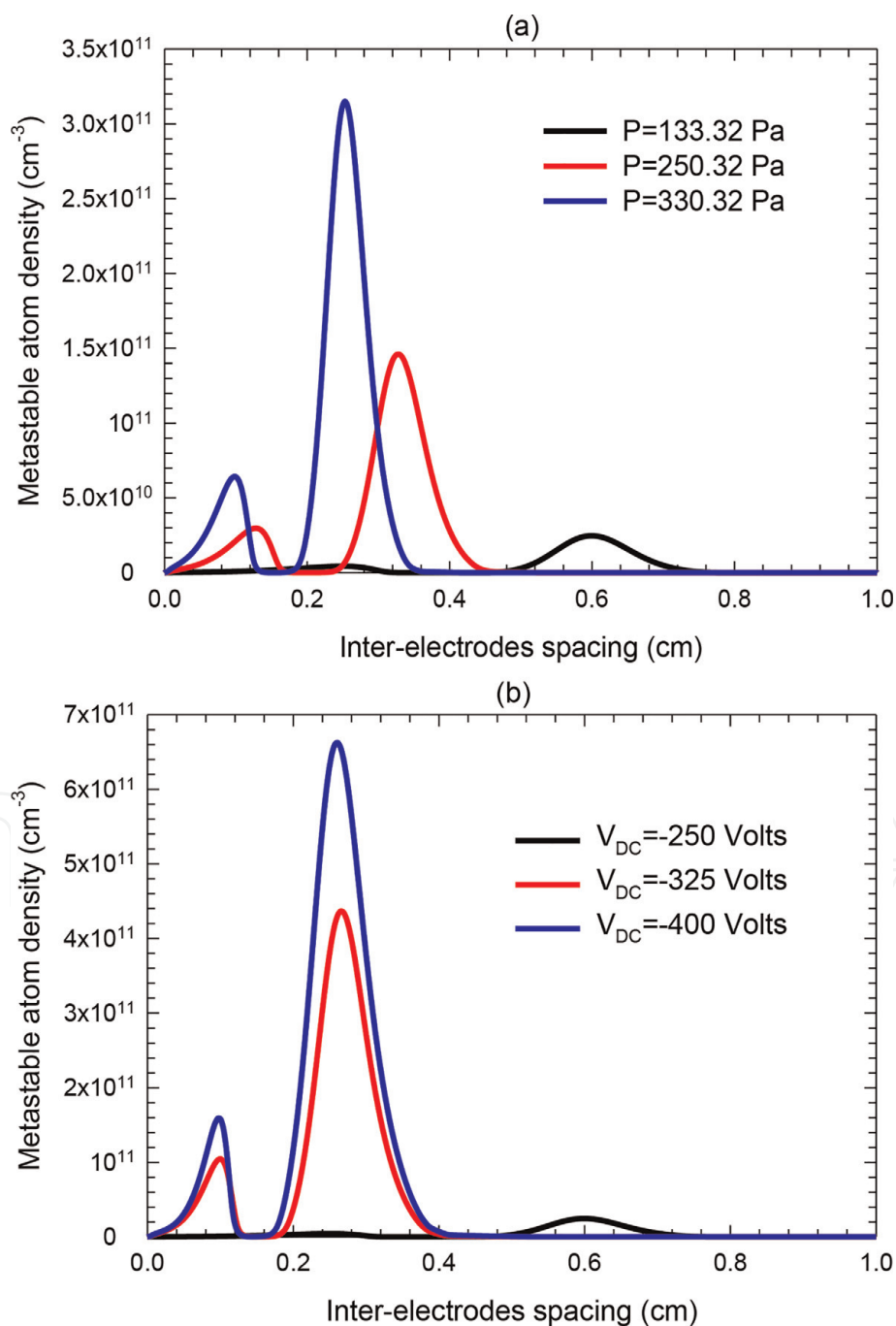


Figure 2. Metastable atom densities as a function of pressure (a) and as a function of voltage (b) in the stationary state in Argon gas.

In the last zone, we remark three dissimilar regions: the anode and the plasma regions and the cathode region. The anode region is characterized by the ion concentration that is less important compared to the electron concentration. In this zone we remark that the convergence of each physical characteristics of the discharge are reached at the time 3.6×10^{-5} s.

3.1 Influence of the voltage and gas pressure

In this part, we will study the influence of the voltage and gas pressure on the argon discharge. So, the potential at the cathode is taking of 250 V and we will alter the gas pressure. For the influence of the applied potential on the discharge, we take the gas pressure at 133.32 Pa. bulk.

Figure 2(a) shows the metastable atoms concentration plots depending on the pressure in the study state. The metastable atoms concentration augments with increasing pressure. For elevated pressure the gas density augments, which the electron diffusion coefficient turns out to be fewer and the bulk of the plasma rises which the both sheaths of the anode and cathode turn out to be small. These circumstances of the charged particle manipulate on the metastable atoms behavior in the study stated, i.e., the cathodic region is overflowing with the electron and metastable atom concentrations, which go faster the ion species in the existence of the electric field.

Figure 2(b) shows the metastable atoms concentration graphs depending on the potential in the study state. For elevated potential the excitation and ionization processes increase, and the charged particle turns out to be raised in the stationary state. Consequently, the metastable atom concentration graphs become growing.

The greatest of the metastable atom concentration varies amidst in 2.47×10^{10} and $6.63 \times 10^{11} \text{ cm}^{-3}$. We judged these results with calculated values established in the literature [9, 10, 12, 15]. Depending on the discharge circumstances, all these value varies amidst in 2×10^{10} and $5 \times 10^{13} \text{ cm}^{-3}$. Consequently, our calculated values something like in the exact range of the size order. We find that the values of

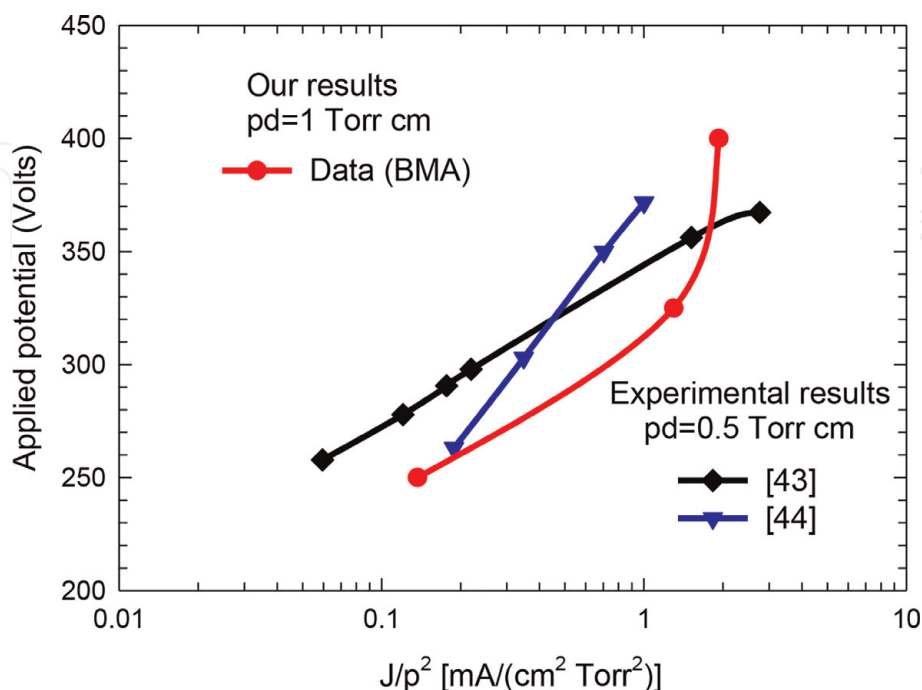


Figure 3. Comparison between the results obtained by our calculation using a database of BMA for $pd = 1$ Torr cm and those given by experimental for $pd = 0.5$ Torr cm in Argon gas.

the current densities are 0.137, 0.508 and 0.843 mA/cm² related to the pressures of 133.32, 250.32 and 330.32 Pa, in that order.

Figure 3 represents the current-voltage properties in the stationary state. The results attained beginning of the database of BMA evaluated to those obtained by experimental method [43, 44]. We find that the results get beginning of the database of the BMA are in excellent conformity judgment against to those experimental results [43, 44].

4. Validity of the model

Figure 4 demonstrates the comparison amidst in our results and those given by Becker et al. [30] (**Figure 4(a)**) ion and electron concentrations, (**Figure 4(b)**) electric field and electric potential, (**Figure 4(c)**) metastable atom concentration and (**Figure 4(d)**) mean electron energy. This figure substantiates the validity of our 1D code. The main dissimilarity amidst in those given by Becker et al. and our results are pointing up in the **Table 2**.

We find that the similar discharge has been studied by Fiala et al. [45], where the hybrid model has been employed in two dimensional configurations. We find that the results got by Fiala et al., it was approximately indistinguishable to our results. In exacting, the maximum of particle concentrations is $1.1 \times 10^9 \text{ cm}^{-3}$ and the electric field at the cathode is 675 V/cm for applying voltage that is equal to 126.3 V. Consequently, the hybrid model is equivalent to our fluid model in the presence of the metastable atom concentrations of these discharge circumstances. Besides our model identifier both properties of the discharge, the mean electron energy and the metastable atom concentrations.

5. Influence for input data of argon abnormal glow discharge

In this part, we will show the properties of the argon plasma discharge in the case of entering data computed by BOLSIG+ software [46]. We remind that the preceding results are obtained with enter data computed by multiterm estimation of the Boltzmann equation. We remind again that the preceding results are identical when are calculated exclusive of the rate coefficients K_m^o and K_m^{io} . The exclusion is the metastable atom concentration, which is prejudiced by these coefficients, i.e., the stepwise ionization processes is insignificant, evaluated to the both ionization of the chemo-ionization and ground state atoms processes. Consequentially, we can calculate the properties of the argon abnormal glow discharge exclusive of K_m^o and K_m^{io} coefficients. The secondary electron emission coefficient is 0.06. The applied voltage at the cathode is -250 V. The gas pressure is 133.32 Pa.

Figure 5 shows the particle density distributions (**Figure 5(a)**), metastable atom concentration (**Figure 5(b)**) and mean electron energy (**Figure 5(c)**) in the stationary state. When we compare between the results given by **Figures 4** and **5**, we conclude clearly the influence of entering data of BOLSIG+ on the characteristics of the argon abnormal glow discharge. In exacting the cathodic region illustrated in the **Figure 4(a)** is totally dissimilar to the cathodic region illustrated in the **Figure 5(a)**. We remind that the similar discharge circumstances (voltage, pressure, etc.) are used in two and multi terms approximations. But, the results are actually dissimilar.

Table 3 gives the main dissimilarity between entering both data of multiterm approximation and of BOLSIG+.

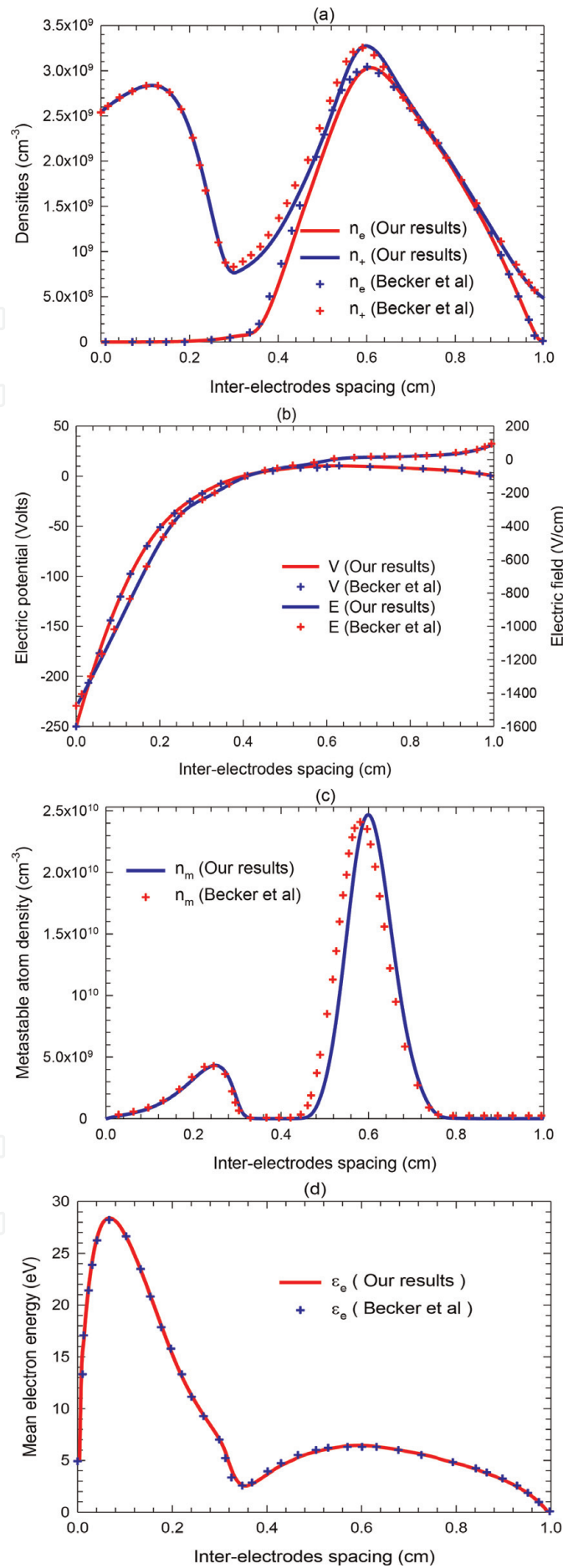


Figure 4. Comparison between our results and those given by Becker et al.: (a) densities, (b) electric potential and electric field, (c) metastable atom density, and (d) mean electron energy in the stationary state in Argon gas.

Becker et al [30]	Our results
Stabilized finite element method for the transport and energy equations are used.	Scharfetter and Gummel scheme is used
The applied potential at the cathode is $V_{DC}(1 - e^{-t/\tau})$ and $\tau = 1$ ns	The applied potential at the cathode is V_{DC}
The steady state is attained at 10^{-4} s	The steady state is attained at 3.6×10^{-5} s
The computations were performed on a 3GHz CPU and typically took about four hours to reach the steady state.	The calculations are carried out in a personal computer. It typically takes about five hours to reach the steady state
The parametric studies are not presented	The parametric studies of gas pressure and applied potential are presented

Table 2.

The major differences between our results and those given by Becker et al.

Figure 6 shows the comparison amidst of the experimental results [47, 48] and our results got beginning database of BOLSIG+ code for $pd = 2$ Torr cm. We remind that the experimental results [47, 48] are given for the diameter of the electrode equal to 8 cm and the inter-electrodes spacing equal to 1 cm. We remind again that the results obtained by Ref. [47] its approximately dissimilar to the results obtained by Ref. [48] due to the experimental circumstances of the secondary electron emission coefficient. We remark that our results got from database of BOLSIG+ code are in excellent accord with the experimental results [47].

5.1 Effect of the metastable lifetime on the characteristics of argon abnormal glow discharge

We remind that the preceding computations are effected through the metastable lifetime equal to $1 \mu\text{s}$ [30], we remind that this value has been proposed by Becker et al. [30]. **Figure 7** represents the effect of the metastable lifetime on the curve of the metastable atom concentration in the study state. For this reason we have used a value of metastable lifetime equal to 56 s of the theories [49] and an experimental value equal to 38 s [50]. We remark that the most of the metastable atom concentration augments from 7.76×10^9 to $2.249 \times 10^{11} \text{ cm}^{-3}$. We note that this effect is noticed just for metastable atom concentration and all characteristic of argon abnormal glow discharge rest unmoved in the study stated. As a consequence, the utilization of the experimental or artificial value of the metastable lifetime has an inconsequential of the abnormal glow discharge characteristics.

6. Characteristics of the neon discharge through entering data of the BOLSIG+

In this part, we will investigate the characteristics of the neon abnormal glow discharge through entering data of the BOLSIG+ code. The gas pressure is 3 Torr. The applied voltage is 300 V. The secondary electron emission coefficient is 0.26 [51]. Additional parameters are declared in the Appendix A. **Figure 8** shows the curves of ion and electron densities (**Figure 8(a)**), metastable atom concentration

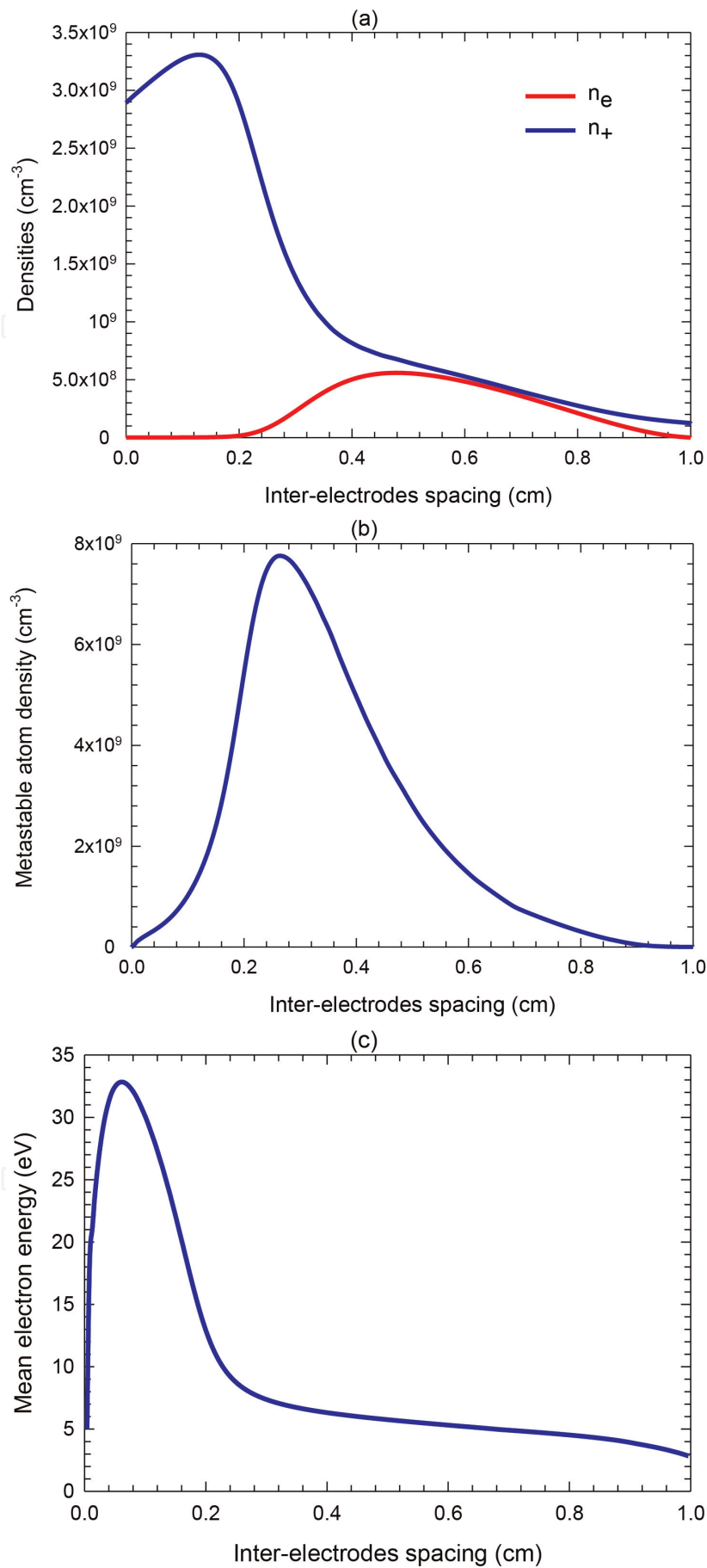
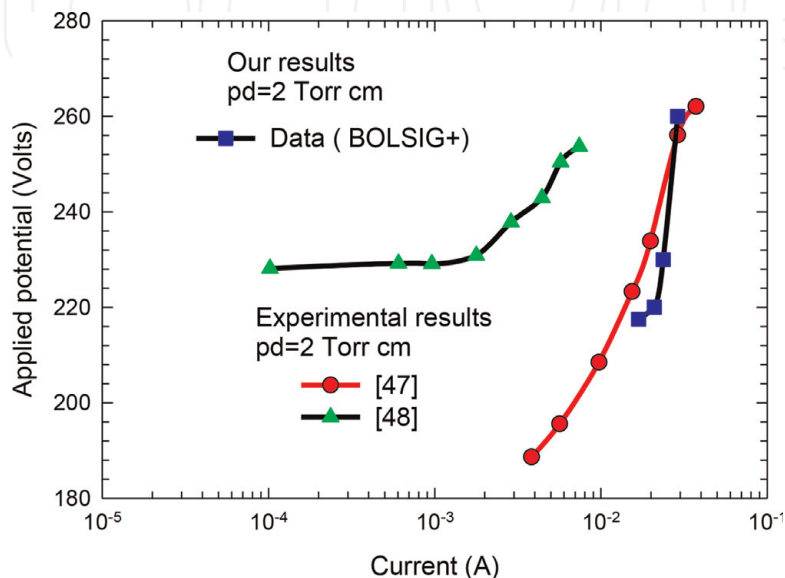


Figure 5. Argon spatial distributions of (a) particle densities, (b) metastable atom density, and (c) mean electron energy in the stationary state for input data of BOLSIG+.

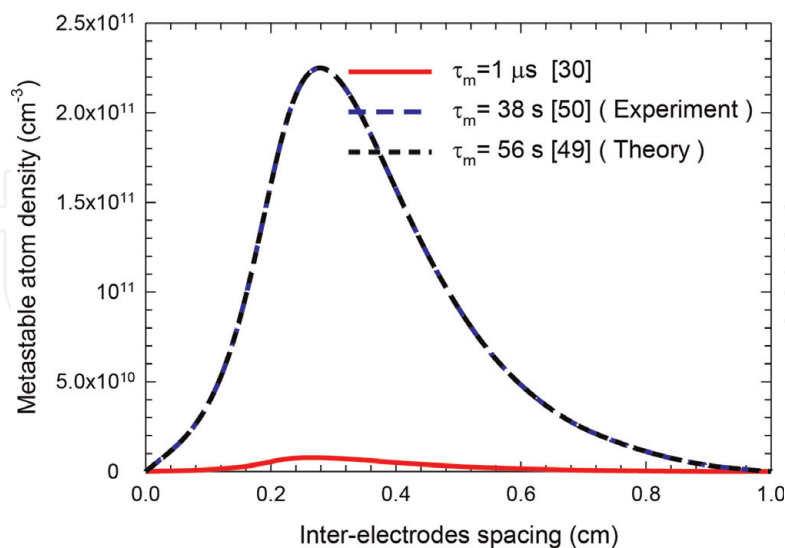
Input-Data (multi term approximation)	Input-Data (BOLSIG+)
Boltzmann equation is solved in the 8-term approximation	Boltzmann equation is solved in the two-term approximation
The activated energy of K_o^m is ≈ 3 eV	The activated energy of K_o^m is $\ll 3$ eV
The activation energy of K_o^{io} is ≈ 5 eV	The activated energy of K_o^{io} is $\ll 5$ eV
Electron mobility is almost great	The electron mobility is great

Table 3.

The major differences between input Data of BOLSIG+ and those given by multiterm approximation.


Figure 6.

Comparison between the results obtained by our calculation using database of BOLSIG+ software for $pd = 2$ Torr cm and those given by experimental for $pd = 2$ Torr cm in Argon gas.


Figure 7.

Influence of the metastable lifetime on the Argon spatial distribution of metastable atom density in the steady state.

(**Figure 8(b)**) and current density (**Figure 8(c)**) depending of the applied voltage in the stationary state. We note that the greatest of the metastable atom concentration is equal to $1.615 \times 10^{11} \text{ cm}^{-3}$. The value of neon current density is 0.1851 mA/cm^2 . The electric field at the cathode achieves the value of 1696.08 V/cm . We note

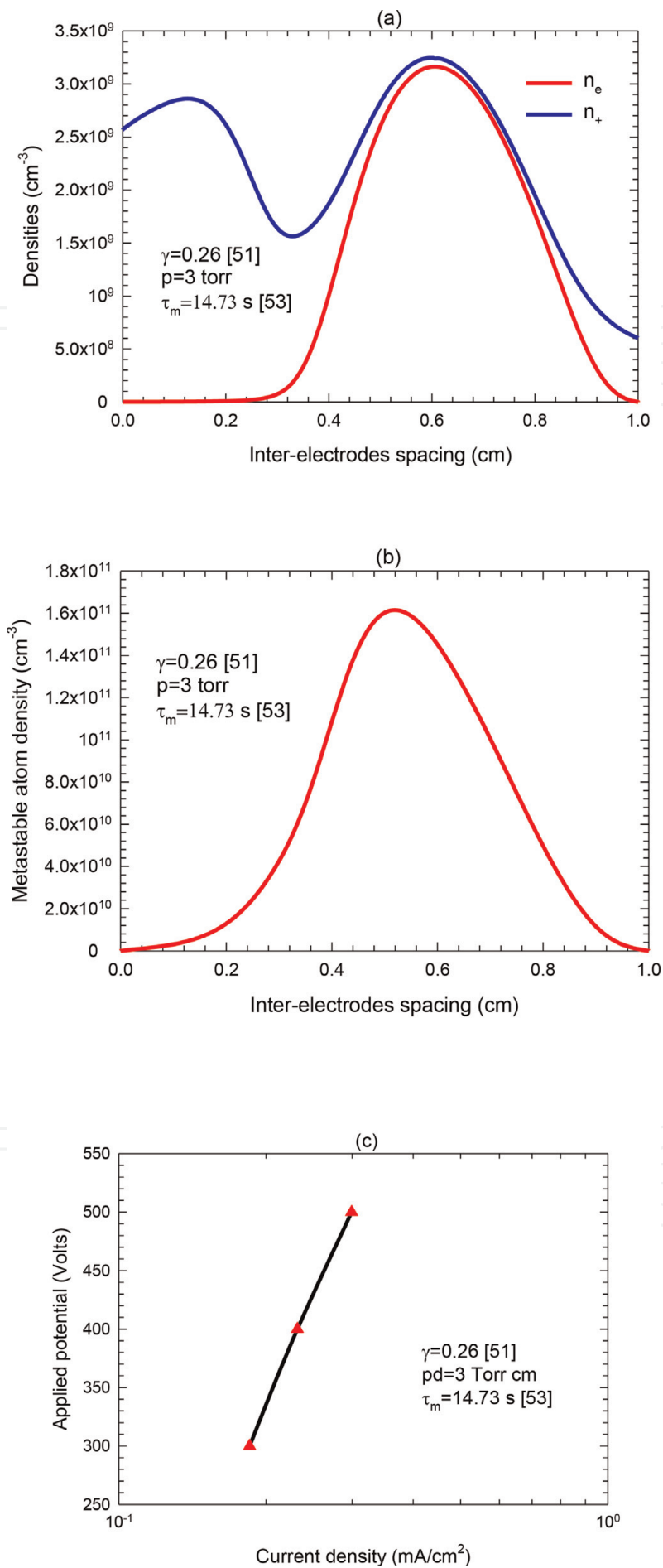


Figure 8. Neon spatial distributions of (a) particle densities, (b) metastable atom density, and (c) current density as a function of applied potential in the stationary state.

that the most of the mean electron energy is 46.30 eV in the cathodic region. As a consequence, the fluid model by injecting the metastable atom concentrations is extremely important for investigating the abnormal glow discharge properties of several pure gases and mixed gas.

7. Conclusion

In order to study the effect of metastable atom density, a second order fluid electric model has been used in the case of a DC low-pressure Ar and Ne abnormal glow discharges. The Poisson equation for the potential and electric field is joined to the first three moments of the Boltzmann's conservation equations ignoring inertia of the charged particles. In the framework of the local energy approximation, the basic data employed in this chapter are calculated by Becker et al. in the case of multiterm estimation of Boltzmann equation (BMA) [30] and from BOLSIG+ software. The task of metastable atom concentration in the discharge is obvious for study into side of plasma glow discharge for several pure gases and mixed gas. We note that the abnormal glow discharge is sustained by secondary electron emission coefficient and the existence of the metastable atom concentration in this particular discharge.

A. Appendix A

The drift velocity of positive ion neon gas is: $w_+ = (11.27E/n) / (1 + 0.01288E/n)^{0.5}$ (m/s) [52] where E/N is in Td. The metastable lifetime of neon gas is equal to 14.73 s [53]. The diffusion coefficient of metastable atoms is $D_m = 150 \text{ cm}^2 \text{ s}^{-1} \text{ Torr}$ [54]. The energy loss of an excited atom is 16.6 eV. The Ionization energy of neon gas is equal to 21.56454 eV. The energy loss (P^{ec}) per electron due to elastic collision of electrons with the background gas is calculated according to [31, 55]. The rate coefficient of chemo-ionization processes is $K_{ci} = 3.6 \times 10^{-10} \text{ cm}^3 \text{ s}^{-1}$ for T = 310 K [56]

Acknowledgements

The authors express their gratitude to Markus M Becker (Greifswald-Germany) for helpful discussions.

IntechOpen

IntechOpen

Author details

Abdelaziz Bouchikhi
Faculty of Technology, Department of Electrical Engineering, University of Saïda,
Saïda, Algeria

*Address all correspondence to: bouchikhiabdelaziz1@yahoo.fr

IntechOpen

© 2019 The Author(s). Licensee IntechOpen. This chapter is distributed under the terms of the Creative Commons Attribution License (<http://creativecommons.org/licenses/by/3.0>), which permits unrestricted use, distribution, and reproduction in any medium, provided the original work is properly cited. 

References

- [1] Ono S, Kato H, Tell S. Simulation and experiment of low-pressure oxygen-nitrogen mixture gas glow discharge plasma. *Combustion Science and Technology*. 1998;**133**:151
- [2] Khomich VA, Ryabtsev AV, Didyk EG, Zhovtyansky VA, Nazarenko VG. Numerical simulation of atomic nitrogen formation in plasma of glow discharge in nitrogen-argon mixture. *Technical Physics Letters*. 2010;**36**:918
- [3] Ponduri S, Becker MM, Welzel S, van de Sanden MCM, Loffhagen D, Engeln R. Fluid modelling of CO₂ dissociation in a dielectric barrier discharge. *Journal of Applied Physics*. 2016;**119**:093301
- [4] Baadj S, Harrache Z, Belasri A. Electrical and chemical properties of XeCl*(308 nm) exciplex lamp created by a dielectric barrier discharge. *Plasma Physics Reports*. 2013;**39**:1043
- [5] Li Q, Zhu X, Li J, Pu Y. Role of metastable atoms in the propagation of atmospheric pressure dielectric barrier discharge jets. *Journal of Applied Physics*. 2010;**107**:043304
- [6] Eckstein EW, Coburn JW, Kay E. Diagnostics of an r.f. sputtering glow discharge - correlation between atomic absorption and mass spectrometry. *International Journal of Mass Spectrometry and Ion Physics*. 1975;**17**:129
- [7] Uzelac NI, Leis F F. Measurement of gas temperatures and metastable state densities in a microwave boosted glow discharge using a diode laser. *Spectrochimica Acta*. 1992;**47B**:877
- [8] Browne PG, Dunn MH. Metastable densities and excitation processes in the He-Cd laser discharge. *Journal of Physics B*. 1973;**6**:1103
- [9] Smith RL, Serxner D, Hess KR. Assessment of the relative role of Penning ionization in low-pressure glow discharges. *Analytical Chemistry*. 1989;**61**:1103
- [10] Strauss JA, Ferreira NP, Human HGC. An investigation into the role of metastable argon atoms in the afterglow plasma of a low pressure discharge. *Spectrochimica Acta*. 1982;**37B**:947
- [11] Ferreira NP, Strauss JA, Human HGC. Developments in glow discharge emission spectrometry. *Spectrochimica Acta*. 1982;**37B**:273
- [12] Ferreira CM, Loureiro J, Ricard A. Populations in the metastable and the resonance levels of argon and stepwise ionization effects in a low-pressure argon positive column. *Journal of Applied Physics*. 1985;**57**:82
- [13] Ferreira CM, Ricard A. Modelling of the low-pressure argon positive column. *Journal of Applied Physics*. 1983;**54**:2261
- [14] Hardy KA, Sheldon JW. Metastable atom density in helium, neon, and argon glow discharges. *Journal of Applied Physics*. 1982;**53**:8532
- [15] Kubota T, Morisaki Y, Ohsawa A, et al. The axial distributions of optical emission and metastable density: comparison between experiments with DC and RF helium glow discharges. *Journal of Physics D*. 1992;**25**:613
- [16] Lymberopoulos DP, Economou DJ. Fluid simulations of glow discharges: Effect of metastable atoms in argon. *Journal of Applied Physics*. 1993;**73**:3668
- [17] Phelps AV, Molnar JP. Lifetimes of metastable states of noble gases. *Physics Review*. 1953;**89**:1202
- [18] Phelps AV. Absorption studies of helium metastable atoms and molecules. *Physics Review*. 1955;**99**:1307

- [19] Ellis E, Twiddy ND. Time-resolved optical absorption measurements of excited-atom concentrations in the argon afterglow. *Journal of Physics B*. 1969;**2**:1366
- [20] Copley GH, Lee CS. Electron excitation and deexcitation coefficients for the 3P_2 , 3P_1 , 3P_0 , and 1P_1 levels of argon. *Canadian Journal of Physics*. 1975;**53**:1705
- [21] Tachibana K. Excitation of the $1s_5$, $1s_4$, $1s_3$, and $1s_2$ levels of argon by low-energy electrons. *Physical Review A*. 1986;**34**:1007
- [22] Kolts JH, Setser DW. Decay rates of $\text{Ar}(4s, ^3P_2)$, $\text{Ar}(4s', ^3P_0)$, $\text{Kr}(5s, ^3P_2)$, and $\text{Xe}(6s, ^3P_2)$ atoms in argon. *The Journal of Chemical Physics*. 1978;**68**:4848
- [23] Den Hartog EA, O'Brian TR, Lawler JE. Electron temperature and density diagnostics in a helium glow discharge. *Physical Review Letters*. 1989;**62**:1500
- [24] Den Hartog EA, Doughty DA, Lawler JE. Laser optogalvanic and fluorescence studies of the cathode region of a glow discharge. *Physical Review A*. 1988;**38**:2471
- [25] Fedoseev AV, Sukhinin GI. Influence of metastable argon atoms and dust particles on gas discharge plasma. *Ukrainian Journal of Physics*. 2011;**56**:1272
- [26] Shumova VV, Polyakov DN, Vasilyak LM. Effect of metastable neon atoms in a positive column of glow discharge with dust particles. *Plasma Sources Science and Technology*. 2014;**23**:065008
- [27] Vasilyak LM, Polyakov DN, Shumova VV. Glow discharge positive column with dust particles in neon. *Contributions to Plasma Physics*. 2013;**53**:432
- [28] Sukhinin GI, Fedoseev AV, Antipov SN, et al. Dust particle radial confinement in a dc glow discharge. *Physical Review E*. 2013;**87**:013101
- [29] Alili T, Bouchikhi A, Rizouga M. Investigations of argon and neon abnormal glow discharges in the presence of metastable atom density with fluid model. *Canadian Journal of Physics*. 2016;**94**:731
- [30] Becker MM, Loffhagen D, Schmidt W. A stabilized finite element method for modeling of gas discharges. *Computer Physics Communications*. 2009;**180**:1230
- [31] Kolokolov NB, Kudrjavitsev AA, Blagoev AB. Interaction processes with creation of fast electrons in the low temperature plasma. *Physica Scripta*. 1994;**50**:371
- [32] Sigeneger F, Winkler R. Nonlocal transport and dissipation properties of electrons in inhomogeneous plasmas. *IEEE Transactions on Plasma Science*. 1999;**27**:1254
- [33] Belenguer P, Boeuf JP. Transition between different regimes of rf glow discharges. *Physical Review A*. 1990;**41**:4447
- [34] Donkó Z. Hybrid model of a rectangular hollow cathode discharge. *Physical Review E*. 1998;**57**:7126
- [35] Marié D, Kutasi K, Malović G, et al. Axial emission profiles and apparent secondary electron yield in abnormal glow discharges in argon. *European Physical Journal D: Atomic, Molecular, Optical and Plasma Physics*. 2002;**21**:73
- [36] Phelps A, Petrović Z. Cold-cathode discharges and breakdown in argon: Surface and gas phase production of secondary electrons. *Plasma Sources Science and Technology*. 1999;**8**:R21
- [37] Bouchikhi A. Two-dimensional numerical simulation of the DC glow discharge in the normal mode and with

- Einstein's relation of electron diffusivity. *Plasma Science and Technology*. 2012;**14**:965
- [38] Becker MM, Loffhagen D. Enhanced reliability of drift-diffusion approximation for electrons in fluid models for nonthermal plasmas. *AIP Advances*. 2013;**3**:012108
- [39] Scharfetter DL, Gummel HK. Large-signal analysis of a silicon read diode oscillator. *IEEE Transactions on Electron Devices*. 1969;**16**:64
- [40] Bouchikhi A, Hamid A, Flitti A, et al. The application of the 2 order fluid model for the townsend's discharge study. *Acta Electrotehnica*. 2008;**48**:404
- [41] Bouchikhi A, Hamid A. 2D DC subnormal glow discharge in argon. *Plasma Science and Technology*. 2010;**12**:59
- [42] Stankov MN, Petković MD, Marković VL, et al. Numerical modelling of DC argon glow discharge at low pressure without and with Ar (3P_2) metastable state. *Romanian Journal of Physics*. 2014;**59**:328
- [43] Stefanović I, Petrović ZL. Volt ampere characteristics of low current DC discharges in Ar, H₂, CH₄ and SF₆. *Japanese Journal of Applied Physics Part 1*. 1997;**36**:4728
- [44] Rozsa K, Gallagher A, Donkó Z. Excitation of Ar lines in the cathode region of a DC discharge. *Physical Review E*. 1995;**52**:913
- [45] Fiala A, Pitchford LC, Boef JP. Two-dimensional, hybrid model of low-pressure glow discharges. *Physical Review E*. 1994;**49**:5607
- [46] Hagelaar G, Pitchford L. Solving the Boltzmann equation to obtain electron transport coefficients and rate coefficients for fluid models. *Plasma Sources Science and Technology*. 2005;**14**:722
- [47] Petrović Z, Jelenković B, Phelps A. *Communication Privée*; 1994
- [48] Jelenković B, Rózsa K, Phelps A. Oscillations of low-current electrical discharges between parallel-plane electrodes. II. Pulsed discharges in H₂. *Physical Review E*. 1993;**47**:2816
- [49] Small-Warren NE, Chow-Chiu LY. Lifetime of the metastable $3P_2$ and $3P_0$ states of rare-gas atoms. *Physical Review A*. 1975;**11**:1777
- [50] Katori H, Shimizu F. Lifetime measurement of the $1s_5$ metastable state of argon and krypton with a magneto-optical trap. *Physical Review Letters*. 1993;**70**:3545
- [51] Chapman B. *Glow Discharge Processes*. New York: John Wiley Sons; 1980
- [52] Frost LS. Effect of variable ionic mobility on ambipolar diffusion. *Physics Review*. 1957;**105**:354
- [53] Zinner M, Spoden P, Kraemer T, et al. Precision measurement of the metastable 3P_2 lifetime of neon. *Physical Review A*. 2003;**67**:010501(R)
- [54] Ricard A. Evolution de la densité des atomes métastables du néon formés dans une décharge à courant continu de faible intensité. *JPHS*. 1969;**30**:556
- [55] Gaens W, Bogaerts A. Kinetic modelling for an atmospheric pressure argon plasma jet in humid air. *Journal of Physics D: Applied Physics*. 2014;**47**:079502
- [56] Sheverev VA, Stepaniuk VP, Lister GG. Chemi-ionization in neon plasma. *Journal of Applied Physics*. 2002;**92**:3454